AMERICAN SOCIETY FOR MICROBIOLOGY | Journal of Bacteriology®

RESEARCH ARTICLE

Phosphosugar Stress in *Bacillus subtilis*: Intracellular Accumulation of Mannose 6-Phosphate Derepressed the *glcR-phoC* Operon from Repression by GlcR

Kambiz Morabbi Heravi,[a] Irfan Manzoor,[b,c] Hildegard Watzlawick,[a] Anne de Jong,[b] Oscar P. Kuipers,[b] Josef Altenbuchner[a]

[a]Institut für Industrielle Genetik, Universität Stuttgart, Stuttgart, Germany
[b]Department of Molecular Genetics, Groningen Biomolecular Sciences and Biotechnology Institute, University of Groningen, Groningen, the Netherlands
[c]Department of Bioinformatics and Biotechnology, Govt College University Faisalabad, Faisalabad, Pakistan

ABSTRACT *Bacillus subtilis* phosphorylates sugars during or after their transport into the cell. Perturbation in the conversion of intracellular phosphosugars to the central carbon metabolites and accumulation of phosphosugars can impose stress on the cells. In this study, we investigated the effect of phosphosugar stress on *B. subtilis*. Preliminary experiments indicated that the nonmetabolizable analogs of glucose were unable to impose stress on *B. subtilis*. In contrast, deletion of *manA* encoding mannose 6-phosphate isomerase (responsible for conversion of mannose 6-phosphate to fructose 6-phosphate) resulted in growth arrest and bulged cell shape in the medium containing mannose. Besides, an operon encoding a repressor (GlcR) and a haloic acid dehalogenase (HAD)-like phosphatase (PhoC; previously YwpJ) were upregulated. Integration of the P_{glcR}-*lacZ* cassette into different mutational backgrounds indicated that P_{glcR} is induced when (i) a *manA*-deficient strain is cultured with mannose or (ii) when *glcR* is deleted. GlcR repressed the transcription of *glcR-phoC* by binding to the σ^A-type core elements of P_{glcR}. An electrophoretic mobility shift assay showed no interaction between mannose 6-phosphate (or other phosphosugars) and the GlcR-P_{glcR} DNA complex. PhoC was an acid phosphatase mainly able to dephosphorylate glycerol 3-phosphate and ribose 5-phosphate. Mannose 6-phosphate was only weakly dephosphorylated by PhoC. Since deletion of *glcR* and *phoC* alone or in combination had no effect on the cells during phosphosugar stress, it is assumed that the derepression of *glcR-phoC* is a side effect of phosphosugar stress in *B. subtilis*.

IMPORTANCE *Bacillus subtilis* has different stress response systems to cope with external and internal stressors. Here, we investigated how *B. subtilis* deals with the high intracellular concentration of phosphosugars as an internal stressor. The results indicated the derepression of an operon consisting of a repressor (GlcR) and a phosphatase (PhoC). Further analysis revealed that this operon is not a phosphosugar stress response system. The substrate specificity of PhoC may indicate a connection between the *glcR-phoC* operon and pathways in which glycerol 3-phosphate and ribose 5-phosphate are utilized, such as membrane biosynthesis and teichoic acid elongation.

KEYWORDS PTS, carbohydrate, mannose, phosphatase, repressor, stress response system

Bacillus subtilis is a soil habitant that is found in different climates. In order to cope with the rapidly changing environment and environmental stresses, e.g., nutrient limitation and changes in temperature and pH, *B. subtilis* has different stress response systems. The stress response systems of *B. subtilis* can be categorized into general and

Citation Morabbi Heravi K, Manzoor I, Watzlawick H, de Jong A, Kuipers OP, Altenbuchner J. 2019. Phosphosugar stress in *Bacillus subtilis*: intracellular accumulation of mannose 6-phosphate derepressed the *glcR-phoC* operon from repression by GlcR. J Bacteriol 201:e00732-18. https://doi.org/10.1128/JB.00732-18.

Editor Tina M. Henkin, Ohio State University

Address correspondence to Kambiz Morabbi Heravi, kambiz.morabbi@iig.uni-stuttgart.de.

Received 26 November 2018
Accepted 14 February 2019
Accepted manuscript posted online 19 February 2019
Published 9 April 2019

specific response systems. The main and general stress response system of *B. subtilis* is the SigB-dependent general response system in which about 150 genes are activated during starvation or a range of stress stimuli, such as cell wall stress, osmotic stress, starvation, and phosphate depletion (1). Depending on the stress stimuli, specific stress response systems can also be activated, e.g., by disturbing the cell envelope structure or metabolic pool. One of the important metabolic pools in *B. subtilis* is the phosphorylated carbohydrates.

B. subtilis uses different systems for the uptake and utilization of carbohydrates. Basically, all of these systems phosphorylate carbohydrates during or after the transport in order to prevent the diffusion of transported carbohydrates into the extracellular milieu (2). In *B. subtilis*, phosphosugars are mainly generated via phosphoenolpyruvate (PEP)-dependent phosphotransferase systems (PTS). During transport via PTS, sugars are phosphorylated by their specific multidomain transporter (or enzyme II [EII]). The intracellular phosphosugar is then converted by a specific enzyme to the glycolysis intermediates (3). Any perturbation in the conversion of transported phosphosugars or elevation of the intracellular concentration of phosphosugars inhibits the cell growth and imposes stress on the cells, e.g., by deletion of *manA* (encodes mannose 6-phosphate isomerase) or *mtlD* (encodes mannitol 1-phosphate dehydrogenase) or overexpression of glucose permease (4–7). Phosphosugar stress disturbs glycolysis pathway by PEP depletion (8).

So far, phosphosugar stress has been studied in *Escherichia coli* and *Salmonella enterica* serovar Typhimurium using nonmetabolizable analogs of glucose, such as methyl α-D-glucopyranoside (αMG) or 2-deoxy-D-glucose (2-DG), and in *Mycobacterium tuberculosis* using mutational studies resulting in accumulation of trehalose 6-phosphate or maltose 1-phosphate (8–11). In *E. coli*, accumulation of intracellular phosphosugar is sensed by a transcriptional regulator, SgrR. The SgrR regulator then induces the expression of a small RNA (sRNA), SgrS (12, 13). Interestingly, *sgrS* also encodes a short peptide, SgrT. Independent of SgrS, SgrT blocks the glucose transport by direct interaction with the glucose PTS transporter PtsG (14, 15). SgrS also downregulates the *manXYZ* mRNA through a dual-base pairing mechanism (reviewed in references 16 and 17). Likewise, SgrS activates the synthesis of YigL, a conserved haloic acid dehalogenase (HAD)-like enzyme, which is a phosphosugar phosphatase (9).

Unlike in *E. coli*, phosphosugar stress has not systematically been studied in *B. subtilis*. Therefore, the phosphosugar stress in *B. subtilis* and the emergence of a specific stress response were investigated in this study. Here, we show that the presence of nonmetabolizable analogs of glucose had no significant impact on *B. subtilis* cell growth and morphology. On the other hand, deletion of *manA* causing accumulation of mannose 6-phosphate arrested the cell growth and resulted in a bulged cell shape. Moreover, the *glcR-ywpJ* (renamed to *phoC*) operon encoding a transcriptional repressor and a HAD-like phosphatase was upregulated in the Δ*manA* mutant during phosphosugar stress.

RESULTS

Phosphosugar stress is generated by deletion of *manA* and *mtlD*. Glucose is the preferred carbohydrate source of *B. subtilis*, which is converted to glucose 6-phosphate (Glc-6P) after its transport. To generate phosphosugar stress by glucose, accumulation of Glc-6P would be possible only after triple deletion of *pgi* (encoding glucose 6-phosphate isomerase for the glycolysis pathway), *pgcA* (encoding α-phosphoglucomutase for cell wall biosynthesis), and *zwf* (encoding glucose 6-phosphate dehydrogenase for the pentose phosphate pathway). However, our attempts to delete *pgi* in the Δ*zwf* mutational background failed. Therefore, the nonmetabolizable glucose analogs, namely, 2-deoxy-D-glucose (2-DG) and methyl α-D-glucopyranoside (α-MG), were used to generate phosphosugar stress similar to previous studies in *E. coli* (12, 18). To do so, strain KM0 (strain 168 with *trp*$^+$) was cultured in LB without or with glucose, 2-DG, and α-MG alone or in combination. Surprisingly, no growth arrest was observed when 2-DG or α-MG was added alone or together with glucose to the medium (Fig. 1A). The growth

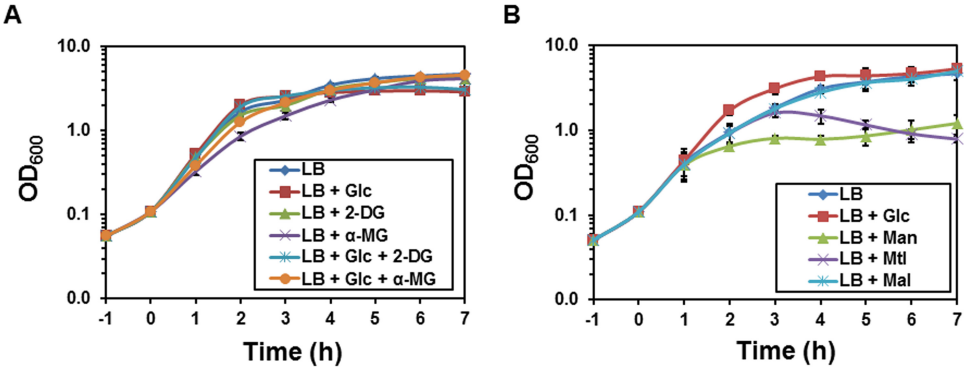

FIG 1 The effect of phosphosugar stress on the growth of *B. subtilis*. (A) Strain KM0 (wild type) was cultured in LB with 0.5% (wt/vol) glucose (Glc), 2-deoxy-D-glucose (2-DG) and methyl α-D-glucopyranoside (α-MG) alone or in combination. The growth of the cells was measured at intervals of 1 h. (B) Strain KM283 (Δ*malA* Δ*mtlD* Δ*manA*) was cultured in LB containing 0.2% (wt/vol) of glucose (Glc), mannose (Man), mannitol (Mtl), or maltose (Mal). All sugars were added at 0 h. All experiments were carried out three times, and the mean values as well as standard deviation (error bars) are demonstrated.

of KM0 in the minimal medium indicated that 2-DG could not be used as the sole carbon source, whereas α-MG could support the growth of KM0 after 24 h (see Fig. S1 in the supplemental material). Unlike *E. coli*, it seems that α-MG and 2-DG cannot cause any growth arrest or abnormal morphology (or phosphosugar stress) in *B. subtilis*. Hence, other carbohydrates were examined in order to stimulate the possible phosphosugar stress systems.

To generate the phosphosugar stress, *malA*, *mtlD*, and *manA* were deleted to block the conversion of maltose 6-phosphate (Mal-6P), mannitol 1-phosphate (Mtl-1P), and mannose 6-phosphate (Man-6P) to glycolytic intermediates. In this way, strain KM283 was constructed carrying the triple Δ*malA* Δ*mtlD* Δ*manA* mutations. Strain KM283 was then cultured in LB medium supplemented with glucose as a control and maltose, mannose, or mannitol, as stressors. The growth of the cells was only retarded in the presence of mannitol and mannose, while glucose had a positive effect on the growth compared with the cells cultured in LB without sugar (Fig. 1B). Surprisingly, the addition of maltose to the medium had no effect on the growth of the cells (Fig. 1B). In fact, further mutations were necessary to generate a weak phosphosugar stress in the presence of maltose (data not shown). The morphology of the KM283 (Δ*malA* Δ*mtlD* Δ*manA*) cells was also monitored by microscope throughout the growth. Interestingly, most of the single cells were club shaped or balloon-like in the presence of mannitol and mannose (Fig. 2), whereas they had a typical rod shape in the presence of glucose or maltose, similar to the medium without sugar (Fig. 2). Overall, the deletion of *manA* and *mtlD* arrested the growth with mannose and mannitol and caused abnormal cell shape as a result of phosphosugar stress.

Phosphosugar stress upregulates the expression of *glcR* and *ywpJ*. To find out whether there are any specific systems responding to the phosphosugar stress, strains KM0 (wild type) and KM283 (Δ*malA* Δ*mtlD* Δ*manA*) were cultured in LB with glucose, mannose, mannitol, or maltose. After 3.5 h of incubation with carbohydrates, the total

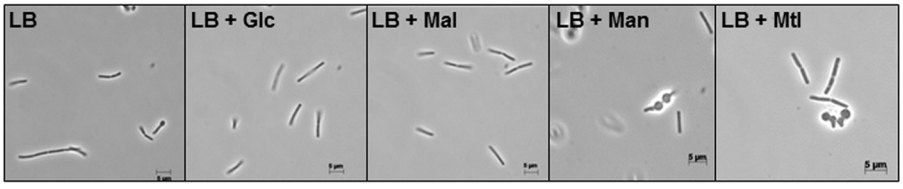

FIG 2 Morphology of the KM283 cells in the presence of 0.2% (wt/vol) glucose (Glc), maltose (Mal), mannose (Man), and mannitol (Mtl) is shown. Strain KM283 was cultured in LB with or without 0.2% (wt/vol) sugars and the samples were collected 3 h after adding sugars.

TABLE 1 Analysis of the transcriptome of the KM0 and KM283 strains in the presence of glucose, mannose, mannitol, or maltose by microarray[a]

Sugar	Upregulated genes	Downregulated gene(s)
Glucose	*manP*, *yqxJ*, *yjdF*	*pyrB*
Mannose	*glcR*, *ywpJ*, *bglH*, *rbsR*, *rbsA*, *rbsD*, *liaI*, *yxiE*	*manA*, *carB*, *pyrK*, *pyrC*, *ldh*, *pyrF*, *mntA*, *pyrE*, *pyrD*, *pyrAA*, *pyrB*, *ptsG*, *glcT*, *mntB*, *gapA*, *pyrP*, *mntC*, *lctP*, *splA*, *flhO*, *pdhB*, *ilvH*, *gcaD* (*glmU*), *serA*
Mannitol	*manP*, *yjdF*, *glcR*, *chr3C* (*ywrA*), *rbsD*, *ywpJ*, *rbsA*, *bglH*, *rbsR*, *rbsB*, *yflS*, *gapB*, *rocA*, *rbsC*, *rbsK*, *rocE*, *bglP*, *citB*, *gutB*, *lytE*, *yxlE*	*mtlD*, *carB*, *mtlF*, *pyrK*, *pyrC*, *mtlA*, *pyrE*, *pyrD*, *pyrF*, *pyrAA*, *alsS*, *ldh*, *splA*, *ilvH*, *leuA*, *pyrB*, *mntA*, *cydA*, *ilvC*, *mntB*, *lctP*, *gapA*, *leuC*, *cydB*, *mntC*, *leuB*, *ahpC*, *ilvD*, *sirA* (*yneE*), *hrcA*, *fbpB* (*ydbN*), *alsD*, *pyrP*, *ilvB*, *hemA*, *fabG*, *sumT*, *ylxY*, *ilvA*, *ahpF*, *pyrG*, *fur*, *hom*, *thrC*, *cggR*, *ymfH*
Maltose	*manP*, *yjdF*, *chr3C* (*ywrA*), *glcR*, *ywpJ*, *yflS*, *bglH*, *ysbA*, *groES*, *rbsD*, *rbsA*, *bglP*, *groEL*, *ysbB*	*malA*, *ptsG*, *glcT*, *ldh*, *mtlF*, *mtlA*, *mntA*

[a]The genes with an upregulation or downregulation in their expression of at least 3-fold in KM283 compared to KM0 expression are listed.

RNA from the cells in different conditions was extracted to be used for microarray analysis. Comparisons of the transcriptome of KM283 with that of KM0 (wild type) revealed genes with 3-fold changes in their expression (upregulation or downregulation) as shown in Table 1 (for further details see Table S4 in the supplemental material). An overview of the upregulated or downregulated genes in different conditions revealed that the downregulated genes were more variable. Nevertheless, four gene clusters, including *mntABCD* (manganese ABC transporter gene), *ptsG* and *glcT* (glucose PTS), *ldh* (lactate dehydrogenase gene), and *pyrBCAKDFE* (pyrimidine biosynthesis), were mainly downregulated under all conditions. As expected, the signals of *manA*, *mtlD*, and *malA* in KM283 were drastically weaker than in the wild-type strain, resulting from their deletion. Surprisingly, the upregulated genes were highly similar in the presence of mannose, mannitol, and maltose, although KM283 did not show a drastic change in its growth with maltose. In detail, three gene clusters were upregulated under all conditions, i.e., *glcR-ywpJ* (glucose catabolite repression), *bglPH* (β-glucoside utilization system), and the *rbsRKDACB* (ribose utilization system) operon. In the case of glucose as a control, only *manP-yjdF* and *yqxJ* (skin element) were slightly upregulated with almost 3-fold induction, whereas *pyrB* was slightly downregulated by 3-fold. The *bglPH* and *rbsRKDACB* operons are catabolic operons; therefore, their upregulation during phosphosugar stress was unclear. All in all, it was assumed that the products of the *glcR-ywpJ* operon (19) consisting of a regulator and a putative phosphatase could be a specific phosphosugar response system. Hence, the *glcR-ywpJ* operon was further investigated.

Only deletion of *manA* leads to upregulation of *glcR-ywpJ*. To better understand the regulation of the *glcR-ywpJ* operon, the promoter region of *glcR* (P_{glcR}) was inserted upstream of *lacZ*. The P_{glcR}-*lacZ* reporter cassette was then integrated into the *amyE* locus of the wild-type strain KM0 constructing strain KM475. The KM475 strain was cultured in LB medium with or without maltose, mannose, and mannitol as the stressors, while glucose, arabinose, or no carbohydrate was added to other cultures (Fig. 3A). Measurement of the β-galactosidase activity indicated a weak β-galactosidase activity (about 25 Miller units) under all conditions. The deletion of *glcR* alone (KM477) or together with *ywpJ* (KM510) resulted in a high level of β-galactosidase activity (about 200 Miller units) under all conditions. The deletion of *ywpJ* (KM479) showed a similar result as that of strain KM475 (wt) having a low level of β-galactosidase activity. These results show that GlcR negatively regulates *glcR-ywpJ* transcription (Fig. 3A).

In order to verify the upregulation of *glcR-ywpJ* during phosphosugar stress, the P_{glcR}-*lacZ* cassette was also integrated into the KM283 strain (Δ*malA* Δ*mtlD* Δ*manA*) constructing KM495. P_{glcR} was induced under all conditions when strain KM495 was cultured in LB regardless of the presence or absence of sugars in the medium (Fig. 3A). Only the presence of glucose reduced the P_{glcR} activity, probably due to the catabolite repression of the genes encoding sugar transporters (Fig. 3A). After deletion of *glcR* and *ywpJ* in the KM283 (Δ*malA* Δ*mtlD* Δ*manA*) strain, strain KM508 was constructed in which a stronger P_{glcR} activity was observed, even in the presence of glucose (Fig. 3A). This experiment confirmed the upregulation of *glcR-ywpJ* during phosphosugar stress.

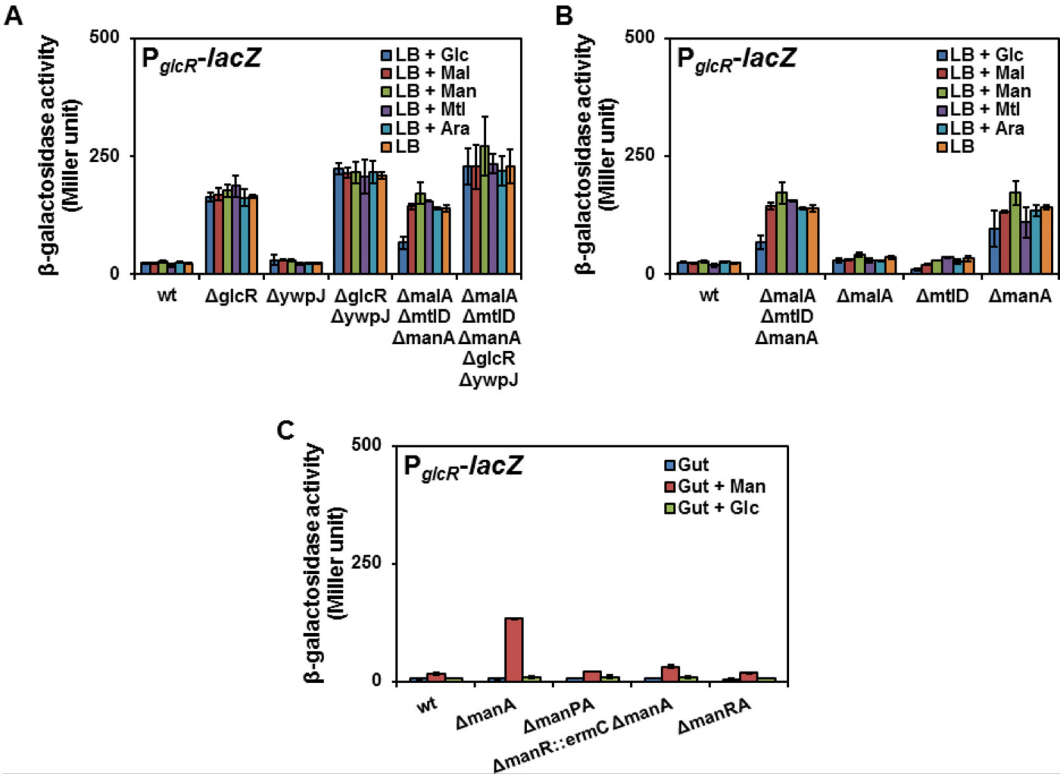

FIG 3 Activity of P_{glcR} in different mutants of *B. subtilis*. (A) Strains KM475 (wt), KM477 (Δ*glcR*), KM479 (Δ*ywpJ*), KM495 (Δ*malA* Δ*mtlD* Δ*manA*), KM508 (Δ*malA* Δ*mtlD* Δ*manA* Δ*glcR-ywpJ*), and KM510 (Δ*glcR-ywpJ*) containing the integrated P_{glcR}-*lacZ* cassette in their *amyE* locus were cultured in LB medium in the presence of different carbohydrates. (B) Strains KM475 (wt), KM495 (Δ*malA* Δ*mtlD* Δ*manA*), KM641 (Δ*mtlD*), KM643 (Δ*manA*), and KM644 (Δ*malA*) having *amyE*::P_{glcR}-*lacZ* were cultured in LB with different carbohydrates. (C) Strains KM475 (wt), KM643 (Δ*manA*), KM647 (Δ*manPA*), KM709 (Δ*manR*::*ermC* Δ*manA*), and KM710 (Δ*manRA*) carrying P_{glcR}-*lacZ* in their *amyE* were cultured in minimal medium with glucitol in the absence or presence of mannose or glucose. All measurements were carried out in triplicates, and the mean value and standard deviations (error bars) were presented here.

However, the reason for the P_{glcR} induction remained unsolved when KM283 (Δ*malA* Δ*mtlD* Δ*manA*) was cultured in LB without sugar.

To find out the reason for the P_{glcR} induction in LB, the P_{glcR}-*lacZ* reporter cassette was integrated into the chromosome of the single-deletion mutants of Δ*manA*, Δ*mtlD*, and Δ*malA* to construct strains KM643, KM641, and KM644, respectively. Interestingly, P_{glcR} was highly active in the Δ*manA* mutant (KM643) regardless of the presence of sugars (Fig. 3B). This suggested that the *manA* deletion mainly results in the upregulation of P_{glcR} in the KM283 strain. To remove the effect of LB, further measurements were carried out in minimal medium containing glucitol, as the basal carbon source, alone or together with mannose or glucose. KM643 (Δ*manA*) cultured in the minimal media showed that P_{glcR} activity is only induced in the presence of mannose. Any disruption in the mannose transport system in the Δ*manA* background, including deletion of *manR* in KM710 or *manP*, encoding the mannose PTS-transporter, in KM647 drastically reduced the P_{glcR} activity (Fig. 3C). Nevertheless, mannose was somewhat able to stimulate the P_{glcR} activity in Δ*manR*::*ermC* Δ*manA* (KM709) probably due to the constitutive expression of *manP* by P_{ermC} (Fig. 3C). Altogether, we assumed that the induction of P_{glcR} in LB depends on mannose PTS and the presence of mannosylated proteins in yeast extract (20).

GlcR represses the *glcR-ywpJ* transcription by binding to the P_{glcR} core elements. In order to understand the regulation of *glcR*, the transcription start site of the *glcR-ywpJ* mRNA was identified by primer extension. The transcription start site was an adenine located 30 bp upstream of the *glcR* start codon (Fig. 4A). Accordingly, the −35 box (TTGAAT) and −10 (TATAAT) box with their 17-bp spacer similar to the consensus

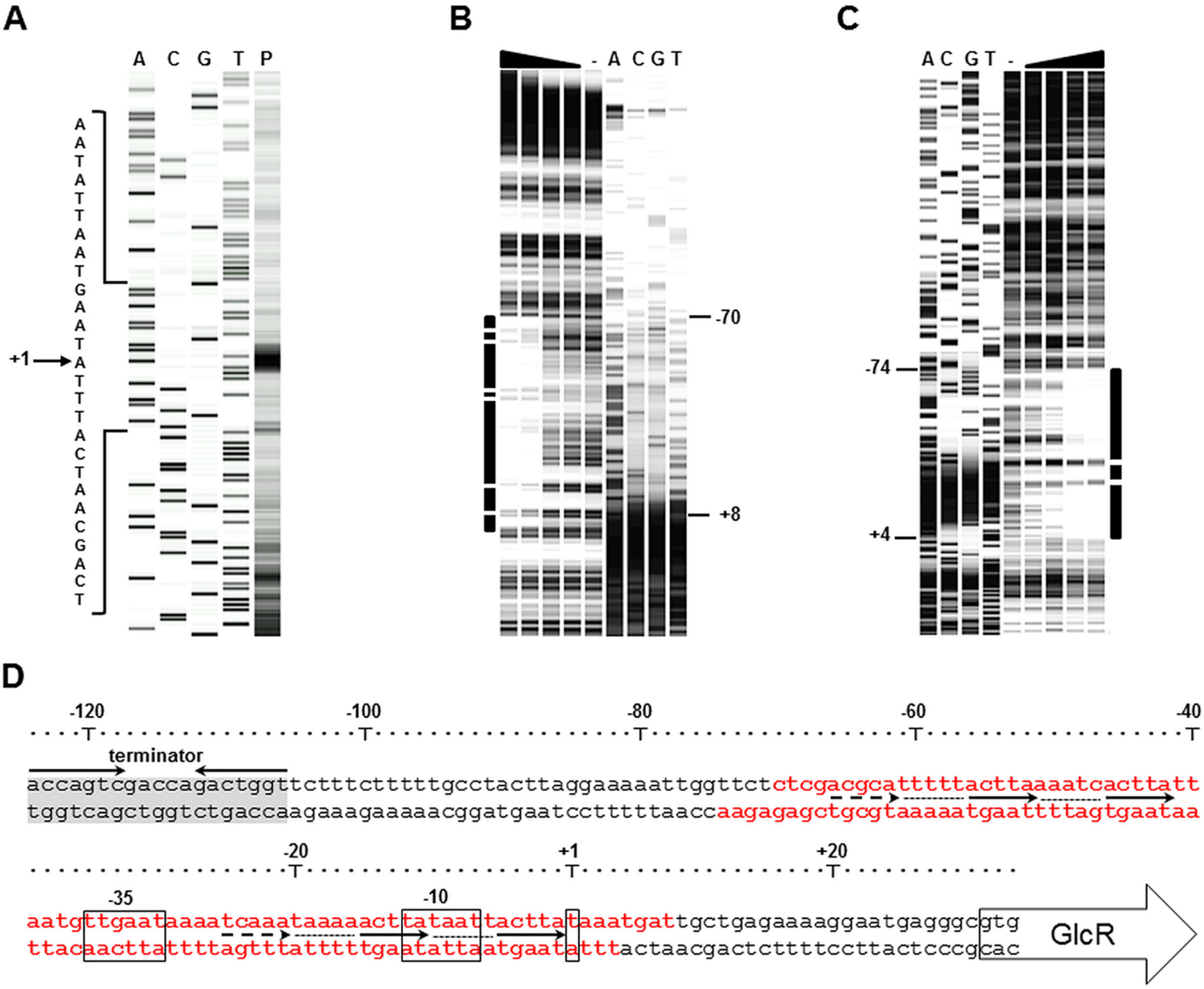

FIG 4 Characterization of the promoter of *glcR-ywpJ*. (A) The transcription start site of *glcR-ywpJ* was identified by primer extension. The sequencing reactions using the dideoxy chain termination method (A, C, G, and T) were compared with the generated cDNA probe (P). (B and C) The DNase I footprinting reactions for 8.6 nM the P_{glcR} coding strand DNA (B) and noncoding strand DNA (C) were compared with the dideoxy chain termination reactions (A, C, G, and T). The DNase I footprinting reactions were performed without GlcR-Strep tag as the negative control (−) or with different amounts of GlcR-Strep tag (0.34, 0.17, 0.08, and 0.04 μM). The solid line shows the protected DNA region in each DNase I footprinting reaction. (D) The DNA sequence of the P_{glcR} region is demonstrated. The promoter core elements (−35 box and extended −10 box) and the transcription start site (+1) are shown by rectangles. The protected DNA region from DNase I is shown by red letters. The solid and dashed arrows indicate the direct repeats of GlcR binding site. The hollow arrow shows the start codon of GlcR. The terminator of the upstream gene *ssbB* is highlighted in gray, and its inverted repeat is shown by arrows.

sequence of the housekeeping sigma factor (σ^A)-type promoters were identified (Fig. 4D). As mentioned before, deletion of *glcR* resulted in the upregulation of P_{glcR}, showing the negative regulation of *glcR-ywpJ* operon by GlcR in an autoregulatory mode of action (Fig. 3A). GlcR has a molecular weight of 28.8 kDa, and it belongs to the DeoR family of transcriptional regulators. To confirm the interaction between P_{glcR} DNA and GlcR by electrophoretic mobility shift assay (EMSA), the Strep-tagged GlcR (both N terminus and C terminus fusions) and GlcR without tag were produced by L-rhamnose-inducible *rha*P_{BAD} in *E. coli* (see Fig. S2A in the supplemental material). All three variants of GlcR were able to interact with P_{glcR} in *E. coli*, repressing the transcription of eGFP by P_{glcR} (Fig. S2B), although Strep tag-GlcR (N terminus fusion) mainly formed inclusion bodies (Fig. S2A). The purified GlcR-Strep tag was able to retard the migration of P_{glcR} DNA in the native-PAGE (see Fig. S3 in the supplemental material). GlcR did not interact with P_{groE} DNA, the promoter of *groE(S/L)*, which was used as a negative control. DNase

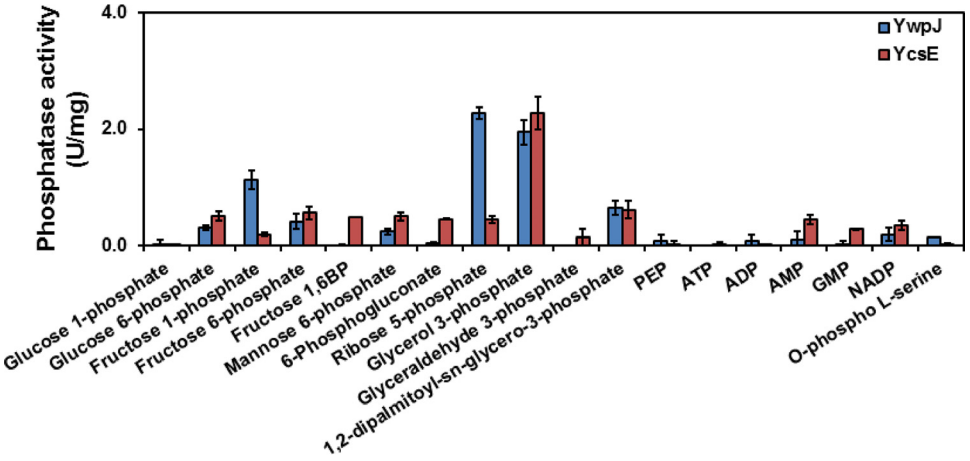

FIG 5 The phosphatase activity of YwpJ and YcsE. Each enzyme reaction was carried out using 1 mM of the substrates in 100 mM sodium acetate buffer (pH 5.7). A total of 2.4 μM YwpJ or YcsE was added to the substrate, and the reaction was stopped after 10 min of incubation at 37°C. The release of the phosphoryl group was detected using malachite green as described in the Materials and Methods. The experiments were carried out at least three times, and the mean values and standard deviation (error bar) were used for presentation.

I footprinting of both coding and noncoding strands of DNA of the P_{glcR} region revealed protected regions between −70 and +8 for the coding strand (Fig. 4B) and −74 and +4 for the noncoding strand (Fig. 4C). Truncation of the 5′ end of the P_{glcR} region indicated that two triple directed repeats of (ACGCA or TCAAA)-N_5-ACTTA-N_5-ACTTA might be the binding sites of GlcR (see Fig. S4 in the supplemental material). Analysis of purified GlcR (without tag) by size exclusion chromatography showed two peaks corresponding to a monomer and a larger complex (larger than hexamer) (see Fig. S5A in the supplemental material). Altogether, these results clearly indicate that GlcR represses its own promoter by binding to the P_{glcR} core elements, causing steric hindrance for the RNA polymerase complex.

YwpJ is an acid-phosphatase-degrading ribose 5-phosphate and glycerol 3-phosphate. The *ywpJ* gene has been predicted to encode a phosphatase. Preliminary studies indicated that YwpJ belongs to the HAD-like phosphatases, which display activities against various intermediates of the central metabolic pathways, glycolysis, and the pentose phosphate pathway. Likewise, a BLAST search of the YwpJ protein sequence showed high similarity to sugar phosphatases YidA and YigL in *E. coli,* both of which are known to degrade phosphosugars. To prove the phosphatase activity of YwpJ, the *ywpJ* gene was overexpressed in *E. coli* JM109 and purified by Strep-Tactin resin. An enzyme assay using *p*-nitrophenyl phosphate (*p*NPP) as a substrate revealed that YwpJ is an acid phosphatase having the highest activity at pH 5.5 and 45°C (data not shown). Likewise, the highest phosphatase activity of YwpJ was obtained using 10 mM $MgSO_4$ in the reaction. Moreover, Mn^{2+} and Co^{2+} were also able to be the cofactors of YwpJ, reaching between 30% to 50% of its maximal activity with 10 mM Mg^{2+} (see Fig. S6A in the supplemental material).

Since *p*NPP is a general substrate for phosphatases, we were interested to know whether YwpJ is able to degrade phosphosugars. Therefore, different phosphorylated substrates, including the glycolysis intermediates, were examined (Fig. 5). The highest activity of YwpJ was obtained in the presence of ribose 5-phosphate (Rib-5P) and glycerol 3-phosphate (Gly-3P). Man-6P was also degraded by YwpJ, albeit significantly weaker than Rib-5P and Gly-3P. Moreover, Glc-6P, fructose 1-phosphate (Fru-1P), and fructose 6-phosphate (Fru-6P) were degraded by YwpJ, whereas other substrates, such as PEP, fructose 1,6-bisphosphate (FBP), 6-phosphogluconate, or glyceraldehyde 3-phosphate, were not degraded by YwpJ (Fig. 5). YwpJ had a K_m between 5 and 9.5 mM for Rib-5P (data not shown), and it had a monomer conformation after purification (Fig. S5A). Altogether, the results indicated that YwpJ is an acid phosphatase (hereafter renamed to PhoC) which mainly dephosphorylates Gly3-P and Rib-5P as its substrates.

GlcR and PhoC are not a specific phosphosugar stress response system. Since PhoC was able to dephosphorylate Man-6P (albeit weakly), it was assumed that deletion of *phoC* could be detrimental for the cells during Man-6P stress, while its expression in the *glcR*-deficient strain might facilitate the bacterial growth during Man-6P stress. To test this hypothesis, *glcR* and *phoC* were deleted alone or in combination in KM283 (Δ*malA* Δ*mtlD* Δ*manA*) and the growth of the constructed strains were investigated in LB without or with mannose and glucose alone or in combination. Surprisingly, deletion of *glcR* or *phoC* had no significant effect on the growth of the cells during Man-6P stress (see Fig. S7 in the supplemental material). This unexpected result indicated that GlcR-PhoC does not function as a phosphosugar stress response system.

To find the possible physiological role of PhoC in *B. subtilis*, its protein sequence was compared with other *B. subtilis* proteins. The protein BLAST revealed the highest PhoC similarity to YwtE and YcsE, both of which are phosphatases of the HAD-like family and are involved in the biosynthesis of riboflavin (21). Also, YcsE was known to have a 5′-nucleotidase activity (22). Therefore, the substrate specificities of YcsE and PhoC were compared. YcsE had its highest activity in the presence of Mg^{2+} under low-pH conditions toward *p*NPP as a substrate (Fig. S6B). Moreover, YcsE had the highest activity toward Gly-3P, which was almost 5-fold stronger than Rib-5P among the phosphorylated carbohydrates (Fig. 5). In contrast to YcsE, PhoC had no or negligible nucleotidase activity with substrates, such as AMP and GMP (Fig. 5). Since the phosphatases are important in the signaling pathways, *o*-phospho L-serine was also introduced to PhoC as a substrate (Fig. 5). Interestingly, the activity of PhoC with *o*-phospho L-serine was only 4% compared without the Rib-5P. Finally, 1,2-dipalmitoyl-*sn*-glycero-3-phosphate was dephosphorylated by both enzymes. Altogether, this showed that PhoC does not have a nucleotidase activity similar to YcsE.

In the final step, finding the inducer of GlcR was of crucial importance in order to clarify the reason for the depression of PhoC during phosphosugar stress. Therefore, dissociation of the GlcR-P_{glcR} DNA complex was studied by EMSA in the presence of different substrates. Surprisingly, Man-6P had no effect on the GlcR-P_{glcR} DNA complex (see Fig. S8 in the supplemental material). On the contrary, Glc-6P, Fru-6P, FBP, and Rib-5P were only able to dissociate the GlcR-P_{glcR} DNA complex at a concentration of 250 mM in the reaction mixture, which was an unlikely physiological condition inside the cytoplasm. Interestingly, EMSA studies revealed that 1,2-dipalmitoyl-*sn*-glycero-3-phosphate (or phosphatidic acid) specifically dissociates the GlcR-P_{glcR} DNA complex at concentrations higher than 5 mM in the reaction (see Fig. S9A in the supplemental material), whereas it showed no effect on the P_{merR} DNA-MerR complex originated from *Streptomyces lividans* (Fig. S9B). Phosphatidic acid is the precursor of phospholipid biosynthesis. This shows that derepression of the *glcR-phoC* during phosphosugar stress could be due to the perturbation in the cell membrane.

DISCUSSION

Prior to this study, the physiological effect of phosphosugar stress on *B. subtilis* was not clear. There were only a few reports showing the elevation in the guanosine pentaphosphate [(p)ppGpp] concentration (stringent response), downregulation of the rRNA encoding genes, and upregulation of *sigX* (an extracytoplasmic sigma factor gene) during phosphosugar stress (7, 23). In our preliminary experiments, we showed that nonmetabolizable analogs of glucose had no effect on the growth of *B. subtilis* (Fig. 1A). Since *B. subtilis* is able to take up α-MG and 2-DG (24–26), it could be assumed that the observed growth in the presence of α-MG and 2-DG may be caused by the activation of a stress response system or enzymes preventing the growth arrest or phosphosugar accumulation. Obviously, the effect of α-MG and 2-DG on the growth of *B. subtilis* needs further investigation. In contrast to α-MG and 2-DG, accumulation of Man-6P and Mtl-1P arrested the growth of *manA*- and *mtlD*-deficient cells and changed their morphology. This abnormality in the morphology of the *manA*-deficient cells (27–29) and *mtlD*-deficient cells was previously observed (6, 30). Despite this growth arrest and

abnormal cell shape, the genes encoding the well-known stress response systems were not upregulated. Apparently, this result does not support the previous studies reporting the upregulation of *sigX* (7) or stringent response (31) during phosphosugar stress. Therefore, a more sensitive approach than microarray, e.g., transcriptome sequencing (RNA-Seq), is necessary to detect the slight changes in the *sigX* or stringent response components.

The upregulated *glcR-phoC* was at first assumed to be a response system for phosphosugar stress because *phoC* was predicted as a putative phosphatase. Nevertheless, at least three observations contradicted this assumption, namely, (i) deletion of the *glcR* and *phoC* genes alone or together had no influence on the growth of the cells during phosphosugar stress (see Fig. S7 in the supplemental material), (ii) the GlcR-P_{glcR} DNA complex was not dissociated in the presence of Man-6P and other phosphosugars *in vitro* (Fig. S8), and (iii) PhoC could weakly dephosphorylate phosphosugars (Fig. 5). Previously, GlcR was reported to play a role in glucose-dependent catabolite repression (32); however, the exact connection of GlcR to the glucose-dependent catabolite repression has not been studied. Likewise, it has been shown that *glcR* belongs to the *comK* regulon (33–35), whereas we saw no effect on the *glcR* expression when *comK* was deleted or overexpressed in the cells (data not shown). The transcriptome analysis by Nicolas et al. (19) showed the separation of the *glcR-phoC* operon from the *ssbB* transcription unit. Therefore, it is likely that the observed *glcR* induction by Berka et al. (34) could be due to the read-through from the induced *ssbB*. Since the derepression of the *glcR-phoC* operon was only dependent on the mannose PTS and the Man-6P accumulation, it is likely that the accumulation of Man-6P has other effects than Mtl-1P, resulting in derepression of *glcR-phoC*.

To understand the physiological role of GlcR and PhoC in *B. subtilis*, it is necessary to find the signal for upregulation of the *glcR-phoC* operon during phosphosugar stress. Our on-going study shows that the perturbation in the cell membrane probably is the signal for the induction of GlcR. This hypothesis came from the results of EMSA showing the interaction between 1,2-dipalmitoyl-*sn*-glycero-3-phosphate and the GlcR-P_{glcR} DNA complex (Fig. S9). Enzyme activity assays revealed that PhoC dephosphorylates Gly-3P and Rib-5P better than other substrates (Fig. 5). This substrate specificity illuminated the probable connection of *glcR-phoC* with other metabolic pathways, such as membrane biosynthesis or teichoic acid elongation, in which Gly-3P and Rib-5P are utilized. Indeed, further studies are necessary for understanding the precise role of GlcR in the physiology of *B. subtilis* and its connection to glucose catabolite repression.

MATERIALS AND METHODS

Bacterial strains, media, and growth conditions. All strains used in this study are listed in Table S1 in the supplemental material. *Escherichia coli* JM109 was used for plasmid propagation, while *E. coli* JM109 and JW2409-1 (Δ*ptsI*::*kanR*) were used for protein production. *E. coli* transformants were selected on LB agar supplemented with ampicillin (100 μg/ml), spectinomycin (100 μg/ml), or kanamycin (50 μg/ml). Unless otherwise specified, all plates were incubated at 37°C. Overexpression of the desired genes was carried out using expression plasmids with L-rhamnose-inducible *rha*P_{BAD}. *E. coli* strains carrying the expression plasmids were inoculated into 25 ml LB containing ampicillin with a starting optical density at 600 (OD_{600}) of 0.05. After 2 h of incubation at 37°C with 200 rpm shaking intensity, 0.2% (wt/vol) L-rhamnose was added to the bacterial cultures. Next, the cultures were harvested after 4 h of incubation at 30°C, and after washing with 100 mM Tris-HCl (pH 7.8), the cell pellets were kept at −20°C for protein purification. To measure the fluorescence intensity, *E. coli* strains carrying plasmid pKAM321 were cultured in 2.5 ml LB medium with kanamycin (for pKAM321) and ampicillin (plasmids expressing *ywpJ*) with a starting OD_{600} of 0.05 at 37°C. L-rhamnose was added after 2 h of incubation, and the strains were further cultured at 30°C. The fluorescence intensity of the cultures was measured after 16 h. Overexpression of *merR* was carried out in *E. coli* BL21(DE3)/pLysS/pJOE971C17 as described before (36).

Bacillus subtilis knockout mutants (BKE) constructed by Koo et al. (37) were obtained from *Bacillus* Genetic Stock center (BGSC; Columbus, OH). *B. subtilis* 168 and its derivative with tryptophan prototrophy, strain KM0, were used as parental strains for construction of the knockout mutants. *B. subtilis* transformants were selected on LB using spectinomycin (100 μg/ml), erythromycin (5 μg/ml), or chloramphenicol (5 μg/ml), depending on the selection marker. For the growth of *B. subtilis* transformants with tryptophan auxotrophy, tryptophan (50 μg/ml) was added to the Spizizen's minimal medium (38). To investigate the bacterial growth, *B. subtilis* mutants were inoculated into 80 ml LB with a starting OD_{600} of 0.05. After 1 h of incubation at 37°C with 200 rpm shaking, different carbohydrates depending on the experiment were added to 10-ml aliquots with a final concentration of 0.2% (wt/vol). The bacterial

growth was then monitored at 1-h intervals. Also, Spizizen's minimal medium without citrate was used for the growth of bacteria. In this way, the overnight cultures were cultured with 0.5% (wt/vol) glucitol, while the main cultures were supplemented with 0.5% (wt/vol) of the desired carbohydrate. The main cultures were started with an OD_{600} of 0.1 and the growth of bacteria was measured every 1 h. The activity of desired promoters in different *B. subtilis* mutational backgrounds was investigated using LB medium supplemented with spectinomycin (100 μg/ml). The overnight culture of each strain was inoculated into 85 ml LB medium with a starting OD_{600} of 0.05. After 2 h of incubation under a shaking condition (200 rpm) at 37°C, the bacterial cultures were divided into 8-ml aliquots and the desired carbohydrates with a final concentration of 0.2% (wt/vol) were added. The β-galactosidase activity of the cultures was measured after 1 h.

Microarray analysis. The effect of the phosphosugar stress on *B. subtilis* was analyzed by microarray using wild-type strain KM0 and triple mutant KM283 (Δ*malA* Δ*mtlD* Δ*manA*). Each strain was inoculated into LB with 1% (wt/vol) of glucose, maltose, mannose, or mannitol with a starting OD_{600} of 0.05. The cells were harvested after 3.5 h of incubation at 37°C and 200 rpm shaking. The procedures regarding the DNA microarray experiment were performed as described previously (39–41). The Genome2D DNA microarray web server was used to obtain microarray data from Agilent slides http://genome2d.molgenrug.nl/ (42). Data analysis was performed by using LimmaR package. The data were normalized using locally weighted scatterplot smoothing (LOWESS) normalization, followed by an in-between-slides quantile normalization. Subsequently, for each array, the quality was examined by adding a weight factor. For differentially expressed genes, a *P* value of <0.001 and false-discovery rate (FDR) of <0.05 were taken for the significance threshold. For the identification of differentially expressed genes, a Bayesian *P* value of <0.001 and a fold-change cutoff of 2 were applied.

Measurement of the phosphatase activity. The phosphatase activity of YwpJ and YcsE were measured according to Lorenz (43). In the preliminary studies, *p*-nitrophenyl phosphate (*p*NPP) was used as a substrate to find the optimal condition, including temperature, pH, and cofactors, for the enzyme activity. After assay optimization, 5 μl of the enzyme (approximately 0.7 mg/ml) was mixed with 10 μl of 250 mM *p*NPP and 35 μl of buffer (100 mM sodium acetate [pH 6.0], 10 mM $MgSO_4$). The reaction was carried out for 10 min at 37°C and stopped by adding 1 ml of 0.4 M sodium borate (pH 9.8). The release of *p*NP was measured at 405 nm. One unit of phosphatase activity was defined as the amount of enzyme catalyzing the liberation of 1 μmol of *p*NP per minute using an extinction coefficient of ε405 (pH 10) of $18.5 \times 10^3\ M^{-1}\ cm^{-1}$ for *p*NP.

To investigate the substrate specificity of YwpJ and YcsE, the release of the phosphate from the phosphorylated substrates was measured according to malachite green method as described by Lorenz (43). To do so, 40 μl of sodium acetate buffer (100 mM, pH 6.0) containing 10 mM $MgCl_2$ was mixed with 5 μl of the enzyme (approximately 0.7 mg/ml) and 5 μl of the desired substrate (10 mM). After 10 min of incubation of the reaction at 37°C, 10 μl of the reaction was mixed with 340 μl ddH_2O. Next, 245 μl solution A (4 vol of 2 M HCl mixed with 3 vol of 100 mM Na_2MoO_4) and 105 μl solution B (0.042% [wt/vol] malachite green in 1% [vol/vol] polyvinylalcohol) were added and the mixture was incubated for 5 min at room temperature. Finally, 700 μl of solution C (7.8% [vol/vol] H_2SO_4) was added and the absorbance was measured at 620 nm. As the blank control, the elution buffer of protein purification was added instead of the enzyme. The absorbance was compared with the standard curve obtained by phosphate standards (0 to 25 μM). One unit was defined as the release of 1 μmol of phosphate per minute.

Measurement of the β-galactosidase activity. Miller's assay (44) was used for measurement of the β-galactosidase activity using *o*-nitrophenyl-β-galactopyranoside (*o*NPG) as a substrate. The enzyme assay using 0.1 ml of the bacterial culture was carried out as thoroughly explained before (45).

Measurement of the fluorescence intensity. The fluorescence was measured in a SpectraFluor microplate reader (Tecan GENios) with 100 μl of samples in a 96-well polystyrene microplate. To standardize fluorescence intensity measurements, bacterial suspensions with an OD_{600} of 0.1 were prepared to monitor eGFP production. The excitation wavelength was 485 nm, and the emission measured at 535 nm with 3 flashes and an integration time of 20 μs.

Methods in supplemental materials. DNA manipulation and plasmid construction, construction of *E. coli* and *B. subtilis* mutants, protein purification by affinity chromatography, determination of the protein molecular weight by size exclusion chromatography, DNA sequencing, primer extension, electrophoretic mobility shift assay (EMSA), and DNase I footprinting are explained in the supplemental material.

Accession number(s). Microarray data have been submitted to the Gene Expression Omnibus (GEO) database under accession no. GSE128187.

SUPPLEMENTAL MATERIAL

Supplemental material for this article may be found at https://doi.org/10.1128/JB.00732-18.

SUPPLEMENTAL FILE 1, PDF file, 1.6 MB.

SUPPLEMENTAL FILE 2, XLSX file, 6.1 MB.

ACKNOWLEDGMENTS

We thank Silke Weber and Gisela Kwiatkowski for their technical assistance throughout the study.

REFERENCES

1. Hecker M, Pané-Farré J, Völker U. 2007. SigB-dependent general stress response in *Bacillus subtilis* and related Gram-positive bacteria. Annu Rev Microbiol 61:215–236. https://doi.org/10.1146/annurev.micro.61.080706.093445.
2. Deutscher J, Galinier A, Martin-Verstraete I. 2002. Carbohydrate uptake and metabolism p 129–150. *In* Sonenshein AL, Hoch JA, Losick R (ed), Bacillus subtilis and its closest relatives: from genes to cells. ASM Press, Washington, DC.
3. Deutscher J, Francke C, Postma PW. 2006. How phosphotransferase system-related protein phosphorylation regulates carbohydrate metabolism in bacteria. Microbiol Mol Biol Rev 70:939–1031. https://doi.org/10.1128/MMBR.00024-06.
4. Wenzel M, Altenbuchner J. 2015. Development of a markerless gene deletion system for *Bacillus subtilis* based on the mannose phosphoenolpyruvate-dependent phosphotransferase system. Microbiology 161:1942–1949. https://doi.org/10.1099/mic.0.000150.
5. Kadner RJ, Murphy GP, Stephens CM. 1992. Two mechanisms for growth inhibition by elevated transport of sugar phosphates in *Escherichia coli*. J Gen Microbiol 138:2007–2014. https://doi.org/10.1099/00221287-138-10-2007.
6. Morabbi Heravi K, Wenzel M, Altenbuchner J. 2011. Regulation of *mtl* operon promoter of *Bacillus subtilis*: requirements of its use in expression vectors. Microb Cell Fact 10:83. https://doi.org/10.1186/1475-2859-10-83.
7. Turner MS, Helmann JD. 2000. Mutations in multidrug efflux homologs, sugar isomerases, and antimicrobial biosynthesis genes differentially elevate activity of the s^X and s^W factors in *Bacillus subtilis*. J Bacteriol 182:5202–5210. https://doi.org/10.1128/JB.182.18.5202-5210.2000.
8. Richards GR, Patel MV, Lloyd CR, Vanderpool CK. 2013. Depletion of glycolytic intermediates plays a key role in glucose-phosphate stress in *Escherichia coli*. J Bacteriol 195:4816–4825. https://doi.org/10.1128/JB.00705-13.
9. Papenfort K, Sun Y, Miyakoshi M, Vanderpool CK, Vogel J. 2013. Small RNA-mediated activation of sugar phosphatase mRNA regulates glucose homeostasis. Cell 153:426–437. https://doi.org/10.1016/j.cell.2013.03.003.
10. Korte J, Alber M, Trujillo CM, Syson K, Koliwer-Brandl H, Deenen R, Kohrer K, DeJesus MA, Hartman T, Jacobs WR, Jr, Bornemann S, Ioerger TR, Ehrt S, Kalscheuer R. 2016. Trehalose-6-phosphate-mediated toxicity determines essentiality of OtsB2 in *Mycobacterium tuberculosis in vitro* and in mice. PLoS Pathog 12:e1006043. https://doi.org/10.1371/journal.ppat.1006043.
11. Kalscheuer R, Syson K, Veeraraghavan U, Weinrick B, Biermann KE, Liu Z, Sacchettini JC, Besra G, Bornemann S, Jacobs WR, Jr, 2010. Self-poisoning of *Mycobacterium tuberculosis* by targeting GlgE in an alpha-glucan pathway. Nat Chem Biol 6:376–384. https://doi.org/10.1038/nchembio.340.
12. Vanderpool CK, Gottesman S. 2004. Involvement of a novel transcriptional activator and small RNA in post-transcriptional regulation of the glucose phosphoenolpyruvate phosphotransferase system. Mol Microbiol 54:1076–1089. https://doi.org/10.1111/j.1365-2958.2004.04348.x.
13. Vanderpool CK, Gottesman S. 2007. The novel transcription factor SgrR coordinates the response to glucose-phosphate stress. J Bacteriol 189:2238–2248. https://doi.org/10.1128/JB.01689-06.
14. Lloyd CR, Park S, Fei J, Vanderpool CK. 2017. The small protein SgrT controls transport activity of the glucose-specific phosphotransferase system. J Bacteriol 199:e00869-16. https://doi.org/10.1128/JB.00869-16.
15. Raina M, Storz G. 2017. SgrT, a small protein that packs a sweet punch. J Bacteriol 199:e00130-17. https://doi.org/10.1128/JB.00130-17.
16. Durica-Mitic S, Göpel Y, Görke B. 2018. Carbohydrate utilization in bacteria: making the most out of sugars with the help of small regulatory RNAs. Microbiol Spectr 6. https://doi.org/10.1128/microbiolspec.RWR-0013-2017.
17. Holmqvist E, Wagner EGH. 2017. Impact of bacterial sRNAs in stress responses. Biochem Soc Trans 45:1203–1212. https://doi.org/10.1042/BST20160363.
18. Kornberg H, Lambourne LT. 1994. The role of phosphoenolpyruvate in the simultaneous uptake of fructose and 2-deoxyglucose by *Escherichia coli*. Proc Natl Acad Sci U S A 91:11080–11083. https://doi.org/10.1073/pnas.91.23.11080.
19. Nicolas P, Mäder U, Dervyn E, Rochat T, Leduc A, Pigeonneau N, Bidnenko E, Marchadier E, Hoebeke M, Aymerich S, Becher D, Bisicchia P, Botella E, Delumeau O, Doherty G, Denham EL, Fogg MJ, Fromion V, Goelzer A, Hansen A, Härtig E, Harwood CR, Homuth G, Jarmer H, Jules M, Klipp E, Le Chat L, Lecointe F, Lewis P, Liebermeister W, March A, Mars RAT, Nannapaneni P, Noone D, Pohl S, Rinn B, Rügheimer F, Sappa PK, Samson F, Schaffer M, Schwikowski B, Steil L, Stülke J, Wiegert T, Devine KM, Wilkinson AJ, van Dijl JM, Hecker M, Völker U, Bessières P, Noirot P. 2012. Condition-dependent transcriptome reveals high-level regulatory architecture in *Bacillus subtilis*. Science 335:1103–1106. https://doi.org/10.1126/science.1206848.
20. Lommel M, Strahl S. 2009. Protein *O*-mannosylation: conserved from bacteria to humans. Glycobiology 19:816–828. https://doi.org/10.1093/glycob/cwp066.
21. Sarge S, Haase I, Illarionov B, Laudert D, Hohmann HP, Bacher A, Fischer M. 2015. Catalysis of an essential step in vitamin B_2 biosynthesis by a consortium of broad spectrum hydrolases. Chembiochem 16:2466–2469. https://doi.org/10.1002/cbic.201500352.
22. Terakawa A, Natsume A, Okada A, Nishihata S, Kuse J, Tanaka K, Takenaka S, Ishikawa S, Yoshida KI. 2016. *Bacillus subtilis* 5′-nucleotidases with various functions and substrate specificities. BMC Microbiol 16:249. https://doi.org/10.1186/s12866-016-0866-5.
23. Samarrai W, Liu DX, White AM, Studamire B, Edelstein J, Srivastava A, Widom RL, Rudner R. 2011. Differential responses of *Bacillus subtilis* rRNA promoters to nutritional stress. J Bacteriol 193:723–733. https://doi.org/10.1128/JB.00708-10.
24. Delobbe A, Haguenauer R, Rapoport G. 1971. Studies on the transport of a-methyl-D-glucoside in *Bacillus subtilis* 168. Biochimie 53:1015–1021. https://doi.org/10.1016/S0300-9084(71)80069-X.
25. Gonzy-Tréboul G, de Waard JH, Zagorec M, Postma PW. 1991. The glucose permease of the phosphotransferase system of *Bacillus subtilis*: evidence for II^{Glc} and III^{Glc} domains. Mol Microbiol 5:1241–1249. https://doi.org/10.1111/j.1365-2958.1991.tb01898.x.
26. Paulsen IT, Chauvaux S, Choi P, Saier MH, Jr, 1998. Characterization of glucose-specific catabolite repression-resistant mutants of *Bacillus subtilis*: identification of a novel hexose:H^+ symporter. J Bacteriol 180:498–504.
27. Elbaz M, Ben-Yehuda S. 2010. The metabolic enzyme ManA reveals a link between cell wall integrity and chromosome morphology. PLoS Genet 6:e1001119. https://doi.org/10.1371/journal.pgen.1001119.
28. Sun T, Altenbuchner J. 2010. Characterization of a mannose utilization system in *Bacillus subtilis*. J Bacteriol 192:2128–2139. https://doi.org/10.1128/JB.01673-09.
29. Wenzel M, Müller A, Siemann-Herzberg M, Altenbuchner J. 2011. Self-inducible *Bacillus subtilis* expression system for reliable and inexpensive protein production by high-cell-density fermentation. Appl Environ Microbiol 77:6419–6425. https://doi.org/10.1128/AEM.05219-11.
30. Watanabe S, Hamano M, Kakeshita H, Bunai K, Tojo S, Yamaguchi H, Fujita Y, Wong SL, Yamane K. 2003. Mannitol-1-phosphate dehydrogenase (MtlD) is required for mannitol and glucitol assimilation in *Bacillus subtilis*: possible cooperation of *mtl* and *gut* operons. J Bacteriol 185:4816–4824. https://doi.org/10.1128/JB.185.16.4816-4824.2003.
31. Henkin TM. 2002. Ribosomes, protein synthesis factors, and tRNA synthetases. ASM Press, Washington, DC.
32. Stülke J, Martin-Verstraete I, Glaser P, Rapoport G. 2001. Characterization of glucose-repression-resistant mutants of *Bacillus subtilis*: identification of the *glcR* gene. Arch Microbiol 175:441–449.
33. Ogura M, Yamaguchi H, Kobayashi K, Ogasawara N, Fujita Y, Tanaka T. 2002. Whole-genome analysis of genes regulated by the *Bacillus subtilis* competence transcription factor ComK. J Bacteriol 184:2344–2351. https://doi.org/10.1128/JB.184.9.2344-2351.2002.
34. Berka RM, Hahn J, Albano M, Draskovic I, Persuh M, Cui X, Sloma A, Widner W, Dubnau D. 2002. Microarray analysis of the *Bacillus subtilis* K-state: genome-wide expression changes dependent on ComK. Mol Microbiol 43:1331–1345. https://doi.org/10.1046/j.1365-2958.2002.02833.x.
35. Hamoen LW, Smits WK, de Jong A, Holsappel S, Kuipers OP. 2002. Improving the predictive value of the competence transcription factor (ComK) binding site in *Bacillus subtilis* using a genomic approach. Nucleic Acids Res 30:5517–5528. https://doi.org/10.1093/nar/gkf698.
36. Brünker P, Rother D, Klein J, Mattes R, Altenbuchner J, Sedlmeier R. 1996. Regulation of the operon responsible for broad-spectrum mercury resistance in *Streptomyces lividans* 1326. Mol Gen Genet 251:307–315.

37. Koo BM, Kritikos G, Farelli JD, Todor H, Tong K, Kimsey H, Wapinski I, Galardini M, Cabal A, Peters JM, Hachmann AB, Rudner DZ, Allen KN, Typas A, Gross CA. 2017. Construction and analysis of two genome-scale deletion libraries for *Bacillus subtilis*. Cell Syst 4:291–305.e7. https://doi.org/10.1016/j.cels.2016.12.013.
38. Anagnostopoulos C, Spizizen J. 1961. Requirements for transformation in *Bacillus subtilis*. J Bacteriol 81:741–746.
39. Afzal M, Manzoor I, Kuipers OP. 2015. A fast and reliable pipeline for bacterial transcriptome analysis case study: serine-dependent gene regulation in *Streptococcus pneumoniae*. J Vis Exp https://doi.org/10.3791/52649.
40. Shafeeq S, Afzal M, Henriques-Normark B, Kuipers OP. 2015. Transcriptional profiling of UlaR-regulated genes in *Streptococcus pneumoniae*. Genom Data 4:57–59. https://doi.org/10.1016/j.gdata.2015.02.004.
41. Manzoor I, Shafeeq S, Kuipers OP. 2015. Transcriptome analysis of *Streptococcus pneumoniae* D39 in the presence of cobalt. Genom Data 6:151–153. https://doi.org/10.1016/j.gdata.2015.08.033.
42. Baerends RJ, Smits WK, de Jong A, Hamoen LW, Kok J, Kuipers OP. 2004. Genome2D: a visualization tool for the rapid analysis of bacterial transcriptome data. Genome Biol 5:R37. https://doi.org/10.1186/gb-2004-5-5-r37.
43. Lorenz U. 2011 Protein tyrosine phosphatase assays. Curr Protoc Immunol Chapter 11:Unit 11.7. https://doi.org/10.1002/0471142735.im1107s93.
44. Miller JH. 1972. Experiments in molecular genetics. Cold Spring Harbor Laboratory, Cold Spring Harbor, NY.
45. Wenzel M, Altenbuchner J. 2013. The *Bacillus subtilis* mannose regulator, ManR, a DNA-binding protein regulated by HPr and its cognate PTS transporter ManP. Mol Microbiol 88:562–576. https://doi.org/10.1111/mmi.12209.